Reliability of Signals From a Chronically Implanted, Silicon-Based Electrode Array in Non-Human Primate Primary Motor Cortex

Selim Suner, Matthew R. Fellows, Carlos Vargas-Irwin, Gordon Kenji Nakata, and John P. Donoghue, *Member, IEEE*

***Abstract*—Multiple-electrode arrays are valuable both as a research tool and as a sensor for neuromotor prosthetic devices, which could potentially restore voluntary motion and functional independence to paralyzed humans. Long-term array reliability is an important requirement for these applications. Here, we demonstrate the reliability of a regular array of 100 microelectrodes to obtain neural recordings from primary motor cortex (MI) of monkeys for at least three months and up to 1.5 years. We implanted Bionic (Cyberkinetics, Inc., Foxboro, MA) silicon probe arrays in MI of three Macaque monkeys. Neural signals were recorded during performance of an eight-direction, push-button task. Recording reliability was evaluated for 18, 35, or 51 sessions distributed over 83, 179, and 569 days after implantation, respectively, using qualitative and quantitative measures. A four-point signal quality scale was defined based on the waveform amplitude relative to noise. A single observer applied this scale to score signal quality for each electrode. A mean of 120 ($\pm$17.6 SD), 146 ($\pm$7.3), and 119 ($\pm$16.9) neural-like waveforms were observed from 65–85 electrodes across subjects for all recording sessions of which over 80% were of high quality. Quantitative measures demonstrated that waveforms had signal-to-noise ratio (SNR) up to 20 with maximum peak-to-peak amplitude of over 1200 μv with a mean SNR of 4.8 for signals ranked as high quality. Mean signal quality did not change over the duration of the evaluation period (slope 0.001, 0.0068 and 0.03; NS). By contrast, neural waveform shape varied between, but not within days in all animals, suggesting a shifting population of recorded neurons over time. Arm-movement related modulation was common and 66% of all recorded neurons were tuned to reach direction. The ability for the array to record neural signals from parietal cortex was also established. These results demonstrate that neural recordings that can provide movement related signals for neural prostheses, as well as for fundamental research applications, can be reliably obtained for long time periods using a monolithic microelectrode array in primate MI and potentially from other cortical areas as well.**

***Index Terms*—Brain–machine interface, chronically implanted, long-term reliability, silicon electrode arrays.**

Manuscript received July 29, 2004; accepted July 22, 2005. This work was supported in part by the Society for Academic Emergency Medicine (SAEM), in part by a Neuroscience Research Fellowship Grant, in part by the Keck Foundation, in part by the National Institute of Neurological Disorders and Stroke (NINDS) Neural Prosthesis Program, NINDS Grant NS25074, and in part by the Defense Advanced Research Projects Agency (DARPA) BioInfoMicro Program.

S. Suner is with the Department of Emergency Medicine and Surgery, Brown University, Providence, RI 02912 USA (e-mail: selim_suner@brown.edu).

M. R. Fellows, C. Vargas-Irwin, and J. P. Donoghue are with the Department of Neuroscience, Brown University, Providence, RI, 02912 USA (e-mail: matthew_fellows@Brown.edu; carlos_vargas_irwin@brown.edu; john_donoghue@brown.edu).

G. K. Nakata was with Brown University, Providence, RI 02906 USA. He is now at 2700 Dolbeer Street, Eureka, CA 95501 USA.

Digital Object Identifier 10.1109/TNSRE.2005.857687

I. Introduction

MANY neurological disorders disrupt the connection between a normal brain and the spinal cord or muscles, preventing voluntary movement. Neuromotor prostheses (NMPs), also termed brain–machine interfaces (BMIs), are promising new devices for paralyzed humans that may provide a route from the brain to external assistive technologies or to the paralyzed muscles themselves. Any NMP will require a sensor to detect neural commands and a means to convert neural signals into a meaningful control output. Recently, proof of concept of such devices was obtained in nonhuman primates. Monkeys achieved immediate and rapid control of a computer cursor in real time by using the neural activity of multiple neurons in the motor cortex (MI) arm area [1]–[3]. Translation of animal-based systems to humans will require a reliable, long-lasting sensor. Although a variety of signal sensors may provide useful neural signals, accurate replication of intended hand motion in external devices appears to require a sensor capable of recording the spiking of neural ensembles. At present, the only means to record such signals is a sensor that is placed very close to the neurons. Acutely placed microelectrodes capable of recording neuron spiking have been available for decades. Such electrodes are ideally fine diameter, pointed-tip conductors that are insulated along their shaft, except at the tip. The fine diameter minimizes tissue damage, while the conical tip shape appears to provide high-quality recordings for reasons that are not fully understood. Adapting single electrodes typically used in experimental neurophysiology to a safe and effective, chronically implantable array has been a formidable task: multiple, chronically implanted electrodes can be damaging to tissue, they can move, and materials can degrade. Challenges in producing such electrodes include control over the array's features, ability to implant using human compatible surgical methods, and adequate insertion methods, as well as their fundamental design.

Normann and collaborators developed a novel 100-electrode array that successfully addresses many of these design features [4]. The array is machined from silicon and etched into 100 identical tapered, platinum-tipped electrodes, each of which is insulated along its length. These electrodes approximate the "ideal" design of standard acute recording microelectrodes. Each is isolated from others at its base by a layer of glass and is fixed within a 10×10 array, with each electrode separated by 400 μm [Fig. 1(b)]. The electrodes are continuous with a planar base which in their aggregate provides a support platform that rests on surface structures. The array is low-profile and made of

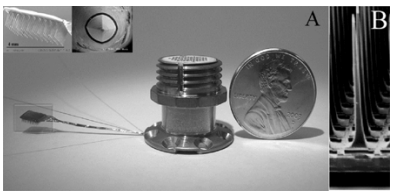

Fig. 1. Array and percutaneous connector assembly. (A) Array, cable and connector. Insets show a higher magnification picture of the array (shown in the black square box magnified by a factor of 25) and a scanning electron micrograph (at 1500 magnification) of one electrode tip. Cut parylene insulation and exposed platinum coated conical tip are clearly visualized in this image. (B) Higher magnification (factor of 200) showing the taper of a single electrode and the base platform that supports the array of electrodes.

biocompatible materials to enhance its stability. This array has been used as a chronically implanted electrode for a number of experimental studies. While recordings have been successfully made for long durations with this array, the recording properties over long times have not been systematically evaluated. In the present study, we report the results of long term recording reliability of the Bionic array in three consecutive monkeys prospectively selected and implanted using human-compatible surgical methods. These three arrays incorporate final designs from a longitudinal development series that has included 39 array implants in 18 monkeys. We demonstrate the ability to obtain extracellular neural signals for at least three months after implantation from arrays in MI and present a set of reliability measures to evaluate the utility of these electrodes for neural prosthesis and research applications.

II. Methods

A. The Array

The Bionic array (as commercially produced by Cyberkinetics, Inc., Foxboro, MA) consists of a 4.4 × 4.2-mm platform with 100 electrodes, of which 96 are available for electrical recording. Electrode spacing is 400 μm and is suitable for recording from surface structures (e.g., cortex) in the central and peripheral nervous system [5], [6]. The electrodes are parylene C coated, boron-doped silicon shanks with Pt-coated conical tips; ~ 40 μm of the tip is exposed (1600 μm^2 surface area; 4180 μm^3 volume) [Fig. 1(a) and (b)], each electrode is electrically isolated from its neighbor by a layer of glass. A wire bundle connects the electrode array to a titanium pedestal that forms a percutaneous connector. The bundle consists of 96, 25-μm gold alloy, polyester-insulated wires, which are collectively coated with silicone elastomer [Fig. 1(a)]. The electrode length used in these experiments was 1 mm. Two Teflon-coated, 75-μm platinum–iridium wires, implanted in the subdural space near the array after stripping approximately 5 mm of the insulation from the tip, serve as reference electrodes. Recording electrodes typically have preinsertion impedances in the range of 100–750 kΩ (measured in 0.9% normal saline solution, 1-nA, 1-kHz sine wave). The preinsertion impedances for the electrodes in the three arrays used in these experiments were 252 kΩ $\pm$ 91 kΩ, 209 kΩ $\pm$ 67 kΩ and 206 kΩ $\pm$ 93 kΩ (mean $\pm$ standard deviation) for monkeys DE, RN, and CL, respectively. The 128 pin percutaneous connector is mounted in a cylindrical titanium case with a flange that is used to attach to the skull via titanium bone screws [Fig. 1(a)]. The connector is coupled to the recording amplifiers with a pressure-fitted screwing mechanism, which utilizes spring-loaded pins to establish electrical contact without insertion forces.

B. Surgical Procedures

Two female (RN and CL) and one male (DE), prospectively selected, *Macaca mulatta* monkeys weighing 4.5–6.0 kg were used for these experiments. Animals were maintained in an Association for Assessment and Accreditation of Laboratory Animal Care, National Institutes of Health (AAALAC, NIH) approved animal care facility. All surgery was performed using standard sterile procedures in an approved animal surgical facility. On the day of surgery, the animal was sedated with ketamine HCl (15 mg/kg), intubated orotracheally, and prepared by shaving the head, and one leg (for an intravenous catheter). Antibiotic (Claforan 50 mg/kg), steroid (dexamethasone 0.5 mg/kg) and analgesic (buprenorphine 0.01 mg/kg) were administered intravenously. The skin was disinfected with a surgical scrub. A stable plane of deep anesthesia was maintained with 1%–2.5% isoflurane through an anesthesia circuit for the duration of the surgical procedure. During the surgical procedure, lactated Ringer's solution was administered at a rate of 5–10 cc/kg/h. Body temperature was maintained at 37 °C–38 °C with a heating pad controlled by a rectal probe. Continuous three-lead electrocardiogram, heart rate, respiratory rate, blood pressure, oxygen saturation (by pulse oximetry), core temperature, expired end tidal carbon dioxide (ETCO_2), ETCO_2 waveform and expired isoflurane concentration were monitored and recorded on a standardized form in regular intervals. After surgery, the monkey was maintained in the recovery area under direct observation until it was observed to be spontaneously moving and able to hold its head upright. Buprenorphine (0.01 mg/kg) for analgesia was administered intramuscularly 8–12 h after the procedure and on subsequent days if there was evidence of discomfort. Antibiotic therapy (Claforan 50 mg/kg) was continued for 5 days. The animal was allowed free access to food and water for one week after the procedure. Experimental trials utilizing behavioral tasks were started only after full recovery from the effects of surgery. In one animal, neural signals were recorded 23 h following array implantation. At this time, the animal exhibited no signs of discomfort, was allowed free access to food and water, and was not required to perform any behavioral tasks during this early postoperative recording session.

1) Array Implantation: After induction of deep anesthesia and prior to surgical preparation and draping, the animal's head was fixed in a standard stereotaxic frame. The skin was incised along the midline or along the occipital scalp with a semi-elliptical incision. The skull was exposed by retracting skin, fascia (the galea aponeurotica), and muscles; the periosteum was then scraped. The percutaneous connector was attached to the skull using eight small pan-head titanium screws. A craniotomy was performed over the motor cortex with approximate coordinates of the rectangular cranial opening 10–18-mm posterior and 8–23-mm lateral, with reference to bregma. The dura was incised and reflected. The array was placed above the cortex in the precentral gyrus at the level of the genu of the arcuate sulcus

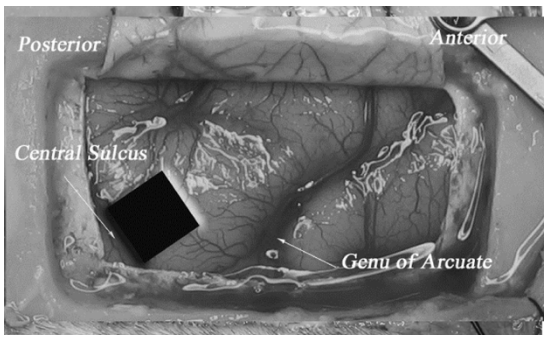

Fig. 2. Craniotomy and location of motor cortex arm area. This representative picture shows the craniotomy site and landmarks used to locate the arm area of primary motor cortex (M1). Dural flap is reflected to expose the cortical surface. Arrows indicate the location of the central sulcus and genu of the arcuate sulcus. Black filled square depicts the location and orientation on the precentral gyrus where the array is positioned for insertion. Animal depicted in this picture was not used in the analysis of data presented in this paper.

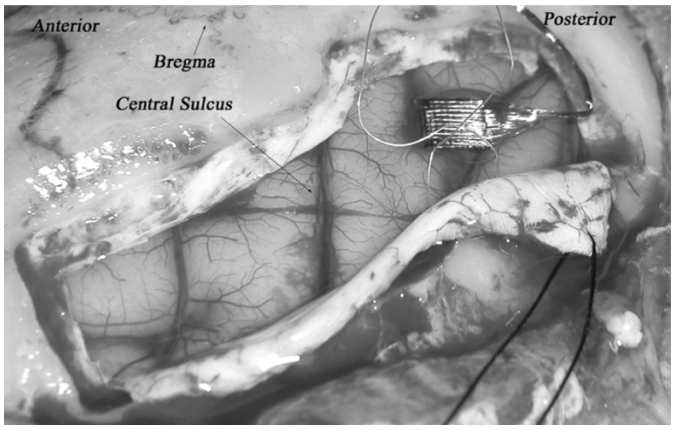

Fig. 3. Craniotomy and an array after insertion. This representative photograph shows an array after insertion into parietal cortex. Anterior direction, central sulcus, and Bregma are depicted in the photograph. Wires seen over the inserted array are the reference wires. This array was placed in parietal cortex and data obtained from this subject is not presented in this paper.

(Fig. 2). An "s" shaped kink was placed in the wire bundle to minimize tethering forces. When positioned at the desired site, the electrodes were rapidly inserted into motor cortex using a pneumatic insertion device (Pneumatic Impulse Inserter, Cyberkinetics Inc., Foxboro MA) (Fig. 3) [7]. The cortical surface and array were then covered with a sheet of sterile Gore-Tex [8]. The dura was reapproximated above the array and sutured in place after the reference wires were inserted in the subdural space. An additional sheet of Gore-Tex was placed over the dura. The bone flap was replaced over the cranial defect and fixed in place with titanium plates screwed to the skull. In monkey CL, the edges of the defect were sealed with sterile medical grade silicon elastomer. In other cases, the defect was filled with silicon elastomer and covered with titanium mesh affixed to the skull with low-profile titanium screws (animals DE and RN). The fascia and skin were reapproximated around the connector in two layers. Three head restraint posts were placed in each animal during a separate earlier surgical procedure, using similar intraoperative methods.

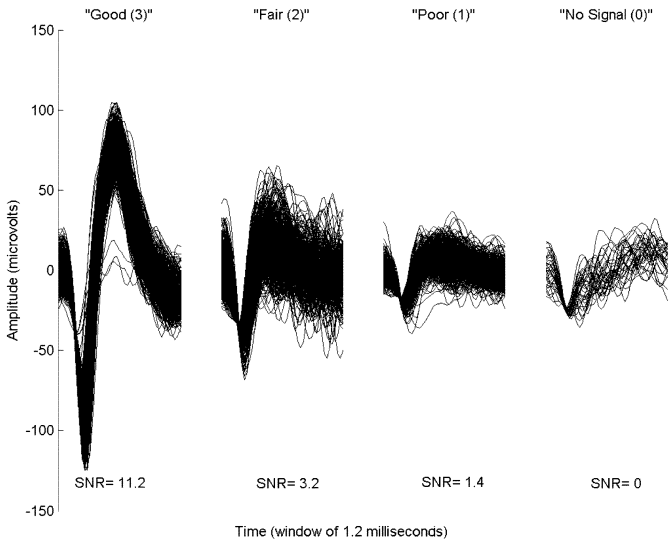

Fig. 4. Signal quality scale. This figure shows examples of waveforms, prior to sorting process, from four different electrodes corresponding to the scale described in the text. From left to right, the signals displayed correspond to "Good (3)," "Fair (2)," "Poor (1)," and "No signal (0)," respectively. y axis is the signal amplitude in microvolts and the x axis for each waveform represents a time window of 1.2 ms. SNR for each waveform is shown at the bottom.

C. Recording Sessions

Recording sessions were conducted periodically to evaluate the signals obtained from each electrode on the array. For recording, the monkey was placed in a custom designed chair and the head was stabilized using a halo that coupled the chair to implanted head posts. Signals from each electrode were recorded continuously and stored during sessions lasting up to 3 h while the monkey performed a learned task. Signals from all the 96 electrodes were recorded and processed simultaneously. Signal quality was initially assessed by a single observer using a predefined four-point scale, in real-time, at the beginning of each recording session while the monkey performed the task in order to provide a qualitative overall impression of the recordings. Signals with at least a biphasic component within the 1.2-ms window that occurred more than 100 times with similar shape were termed as neural "waveforms." The term waveform is used to define a repeatable biphasic signal without judgment as to whether this is a signal from one single neuron. Overall stability and uniformity of waveform shape compared to other waveforms or noise across the recording session was the major criterion that a single unit was being recorded. The signal quality scale was defined as (Fig. 4).

Good signal (3): Able to set a threshold to detect one or more waveforms of unique shape from the signal above the background. The waveforms in these signals are easily distinguished with the naked eye without any signal processing or special sorting. Generally, these signals were later verified to have signal-to-noise ratio (SNR) above 4.
Fair Signal (2): Able to set a threshold to detect and sort at least one waveform from the signal. The waveforms in these signals are less easily distinguished from others in the recording, but the confidence of being able to sort unique waveforms is high. These signals typically have SNR between 2 and 4.

Poor signal (1): Able to identify mixed waveforms contained in the signal. It is not possible to identify unique waveforms in these signals with the naked eye and the confidence of being able to sort units is low. These signals generally have SNR less than 2.
No signal (0): Unable to distinguish signal from background noise or a faulty electrode. SNR for these signals is less than 1 or the signal consists of waveforms identified as originating from a nonbiological source such as 60-Hz interference.

D. Data Acquisition

Signal processing was performed using commercial hardware and software (Multichannel Acquisition Processor, Plexon Inc., Dallas, TX). The signals were processed by a head stage with unity gain for impedance matching then amplified in two stages up to 36 000 times (user-defined range 1000–36 000). Final gain was controlled by software. Signals were further processed with 80-Hz two-pole low-cut and 8-kHz six-pole high-cut filters. Data were recorded from 96 channels simultaneously with 40-kHz analog-to-digital conversion and 12-bit resolution on each channel. Behavioral event codes were recorded on a digital input as a strobed word with time-stamp accuracy of $\sim 150\ \mu$s. Data were stored on a personal computer and archived using a DVD system.

E. Impedance Measurements

In vivo impedance was measured periodically in the alert monkeys using a commercial impedance meter designed for microelectrodes (Electrode Impedance Tester, Model IMP-1, BAK Technologies Inc., Germantown, MD), for each electrode in two monkeys. The device applies a 1000-Hz, 1-nA sine wave to measure impedance.

F. Operant Conditioning

To evaluate movement-related signals from recorded neurons, three monkeys were trained to perform an eight-direction (0°–315° in the frontal plane; 0° to the right) instructed-delay, reaching task using a button-box. The button-box, placed ~ 20 cm in front of the monkey's eyes, consisted of a center button surrounded by eight identical buttons equally spaced around the center in a circle with a diameter of 143.7 mm. Each 19.6-mm-diameter button contained a red light-emitting diode (LED) that illuminated the button. Monkeys were trained to press and hold the center button using the digits of their right hand (contralateral to the implanted array). When this was accomplished, one of the surrounding buttons was lit for 150 ms. The monkey learned to hold the center button, remember which button was lit. When a "go" cue was given (by lighting all the buttons simultaneously), the monkey was required to press the target button to receive a juice reinforcer. Timing of the light signals and button activations were directed to the signal processing system, which logged the time of these events with respect to the recorded neural activity. The custom design of the button-box control software allowed manipulation of reward variables and task parameters to minimize training time.

G. Data Analysis

Data were recorded, digitized, and stored on personal computers as spike timestamps and waveforms (during 1.2 ms) along with synchronized behavioral information. Any waveform which crossed a predetermined threshold was saved and used for offline analysis. The threshold was set individually by the investigator, low enough to maximize the capture of all likely waveforms. Action potentials from each electrode were then classified using offline spike-sorting software, which utilizes template sorting algorithms (Offline Sorter, Plexon Inc., Dallas, TX). Classified signals were analyzed by construction of average waveforms, calculation of SNR, peri-event rasters, histograms, and reach-direction tuning. The global reliability of the array was assessed by calculating the yield after each recording session (yield = number of electrodes with identifiable waveform/total number of electrodes on the array). In addition, various characteristics of the signal, such as principle component dispersion and inter-spike interval, from each electrode were evaluated as a function of intervening time as additional measures of reliability.

1) Offline Sorting: Stored signals were sorted into similar waveform shapes using commercial software (Offline Sorter, Plexon Inc., Dallas, TX) by the same single investigator, in an attempt to identify and isolate those waveforms that represented single units. The sorting techniques were similar to those detailed in prior studies [9]. Sorted data were then analyzed using waveform shape and unit firing characteristics. Rasters, histograms, preferred directions, SNRs, and inter-spike interval curves were calculated using a combination of commercial (NeuroExplorer, NEX Technologies, Littleton, MA) and custom software (developed utilizing MATLAB, Mathworks, MA).

2) SNR Calculation: As a quantitative measure, SNRs were calculated using the following formula:

$$\mathrm{SNR} = \frac{A}{(2 * \mathrm{SD}_{\mathrm{noise}})}$$

where A, the amplitude, is the peak-to-peak voltage of the mean waveform, and $\mathrm{SD}_{\mathrm{noise}}$ is the standard deviation of the noise. Amplitude A and noise ε were calculated as follows.

Each waveform w is a vector of N voltage samples, each collected at some time τ relative to a threshold crossing

$$w^i = \left[v^i(\tau_1), v^i(\tau_2), \ldots, v^i(\tau_N)\right].$$

The collection of all k waveforms for that unit is then

$$W = \begin{bmatrix} v^1(\tau_1), v^1(\tau_2), \ldots, v^1(\tau_N) \\ \vdots \\ v^k(\tau_1), v^k(\tau_2), \ldots, v^k(\tau_N) \end{bmatrix}.$$

The mean waveform, $\overline{W}$, is the average of W taken down the columns, $\overline{W} = W^T Z$, where Z is a $k \times N$ matrix in which each element is $1/k$.

The amplitude, A, is then, $A = \max(\overline{W}) - \min(\overline{W})$.

The noise, ε, is obtained by subtracting the mean, $\overline{W}$, from each individual waveform

$$w^i, \varepsilon = W - \begin{bmatrix} \overline{W}^T \\ \vdots \\ \overline{W}^T \end{bmatrix}$$

where $(-)$ is element-wise subtraction and T represents the transpose operator.

$\mathrm{SD}_{\mathrm{noise}}$, then, is the standard deviation taken over all values in ε, irrespective of their position in the matrix. In other words, for a given cell, ε is just the collection of residuals when the mean waveform is subtracted from each individual waveform; and $\mathrm{SD}_{\mathrm{noise}}$ is the standard deviation over this collection.

3) Waveform Reliability: Changes in the unit composition for each electrode over time were quantified using two different relative measures. One involves the distance between centers of principal component (PC) clusters, the other, distances between ISI distributions (Fig. 15). For each electrode, a reference unit was chosen. Both the PC and ISI measures are in terms of distances to the reference unit. Each "reference" unit was chosen as the unit with the highest SNR on the day closest, on average, to all the other recording days for which there was at least one unit on that electrode.

PC distance. For each electrode, the standardized distance between the center of the principal component cluster for the reference unit and the center of the PC cluster for each other unit was calculated as a function of intervening days for all electrodes with > 200 waveforms and $\mathrm{SNR} > 3.0$. Standardized distance is defined in terms of the standard deviation in each of four dimensions (the first four PCs were used) of the reference cluster. Formally, this produces a four-dimensional (4-D) vector of standardized distances. It is the magnitude of this vector which we report. Therefore, a cluster one unit of distance from the reference cluster is one standard deviation away its center. This simultaneously provides a statistical measure of distance (distance in terms of dispersion) and allows for comparison across channels and units through normalization.

ISI distance. Distances between ISI distribution curves for each unit on given electrodes was calculated as a function of intervening days between recording sessions. The distance reported is the maximum distance between the cumulative distribution function of the reference ISI distribution and the ISI distribution of the unit to which it is being compared. This measure is identical to the Kolmogorov–Smirnov statistic for comparing two distributions. The ISI was displayed as a cumulative probability function (Fig. 15).

4) Preferred Direction Calculation: Preferred direction was calculated to measure the reliability of target directed movement relationships of recorded waveforms. The preferred direction of a sorted unit was calculated using a 500-ms window centered on the initiation of movement to a peripheral target. Only successfully rewarded (completed) trials were used. A least squared error cosine fit was utilized to establish directional tuning. Only the units which did not have statistically similar firing rates for all directions (one-way analysis of variance, $\mathrm{ANOVA} < 0.05$) were used in the analysis.

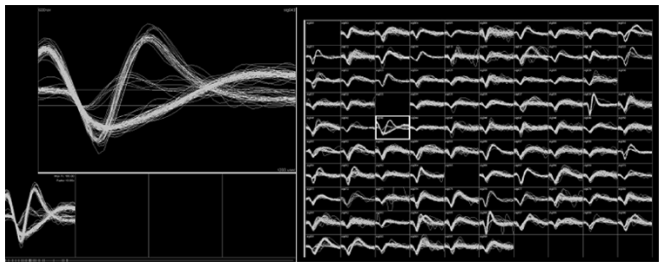

Fig. 5. Waveforms obtained during simultaneous recording from 96 electrodes. Right portion of the image shows waveforms from all 96 electrodes displayed simultaneously in real-time. Left half shows an enlarged image of selected channel. Channel selected in this image is outlined with a white rectangle (Channel 42). At least two separate action potential waveforms can be seen in this example. Arrangement of the signals from the array electrodes displayed in this image does not correspond to the spatial location of the electrodes on the array.

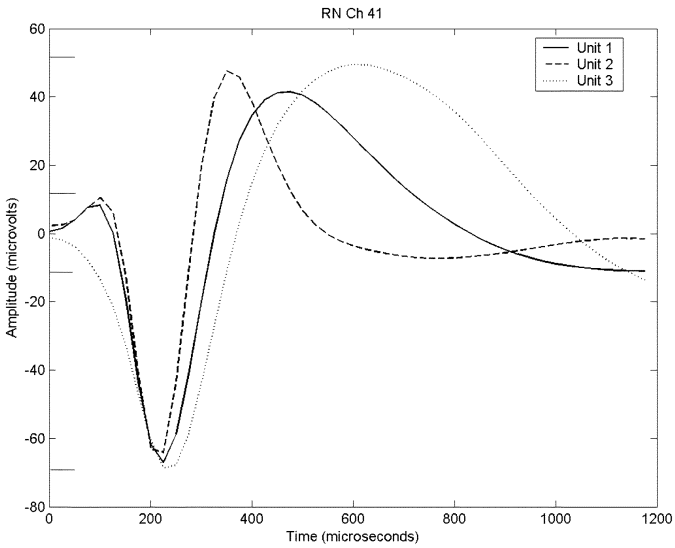

Fig. 6. Representative example of three separate units recorded from a single channel. Three mean waveforms (each an average of 500–10 000 individual waveforms) from a single electrode recorded during the third session from one monkey (RN) are shown in this figure. x axis indicates time in microseconds and y axis waveform amplitude in microvolts). Signal and noise amplitudes are marked with horizontal lines on the y axis. Outer two lines show signal amplitude and the inner two lines level of noise. SNR for these waveforms was 5. These separate units were sorted using the techniques described in the text.

III. Results

The results describe the general recording characteristics of the array, followed by qualitative and then quantitative measures of reliability. We then describe movement related activity. Finally, we compare our findings with observations from recordings made in earlier arrays, as well as results from recordings attempted from arrays placed in the parietal cortex.

A. General Recording Characteristics

Fig. 5 shows representative mean waveforms obtained across during a typical recording session (monkey RN). Across the animals, a mean of 75–90 channels contained waveforms of sufficient amplitude to be triggered above background noise (Fig. 7). The remaining channels had no waveforms which regularly exceeded background noise, which may reflect a

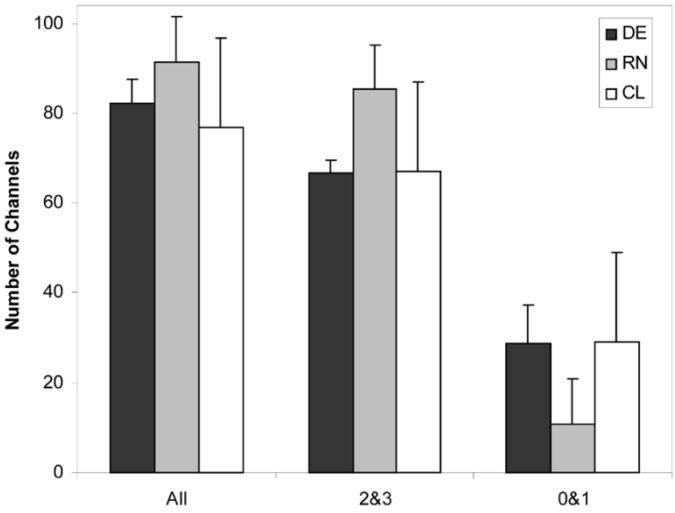

Fig. 7. Mean number of channels with signals from three monkeys. The y axis denotes the number of electrodes on an array with signal (max 96). Different shades of grey represent different study animals (black: DE, grey: RN and white: CL). Three separate groupings on the x axis represent all signals (All), electrodes with fair plus good signal (2 and 3), and electrodes with no signal plus poor signal (0 and 1) from left to right. Error bars denote standard deviation.

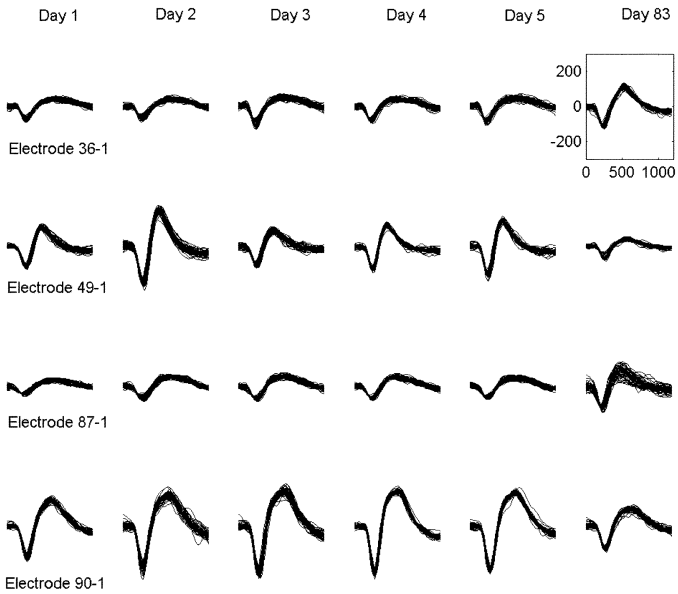

Fig. 8. Representative example of waveform shapes. Eighteen waveform shapes (each depicting 50 superimposed classified waveforms) on four separate electrodes during six different recording sessions from one monkey (RN) are shown in this figure. Each recording session is designated by a column and is labeled at the top (day 1–day 83). Each separate electrode is displayed in a row and is labeled on the left (electrode 36-1, electrode 49-1, electrode 87-1, and electrode 90-1). Scale indicated on the top right waveform (x-axis, time: 0–1200 μs; y-axis, amplitude: -300–300 μv) applies to all waveforms in this figure.

remote location of the recording tip from a cell. Several channels often had multiple waveforms of different shapes and amplitudes; rarely there were up to four separable waveforms on a single channel. Examples of waveform characteristics for multiple different waveforms obtained from a single electrode are displayed in Fig. 6. The maximum action potential peak-to-peak amplitude observed was 1.2 mV and the best SNR on an electrode was greater than 20. The majority of electrodes provided "good" signal quality, as defined in the methods section. From 68%–89% of channels contained signals which were categorized as ***good*** or ***fair*** (Fig. 7). Across the three monkeys, using spike sorting methods, 119 ± 17, 146 ± 7, 120 ± 18 (mean $\pm$ SD) units were identified from the signals obtained from 96 electrodes (mean $=$ 1.3 units/electrode). The total number of units recorded from the three monkeys over all recording sessions was 719, 1298, and 2683 for DE, CL, and RN, respectively (total recording sessions multiplied by the number of discriminated waveforms on all electrodes per session). This total could include mixtures of the same or different neurons because we did not specifically evaluate measures that could determine whether the same neurons were present each day. However, we found that shape of the action potential waveform was similar 38% of the time spanning 91 days in one animal (CL), although it must be noted that wave shape is a poor measure of consistency since the same neuron could have many action potential shapes over time (with shifts in electrode position) and similar wave shapes can be generated by different neurons. Other criteria must be applied to address this issue. This will be the subject of future studies. The appearance of wave shapes recorded on the same electrode over time can be appreciated in Fig. 8, which demonstrates that similar waveform can be present for many days.

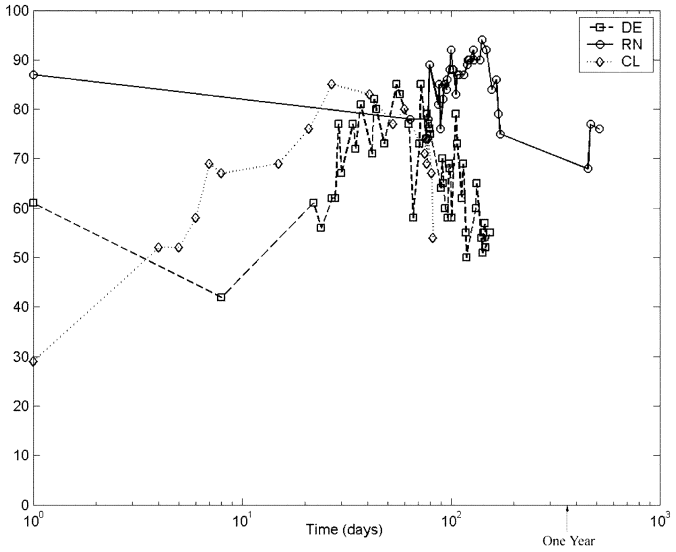

Fig. 9. Number of *good* or *fair* waveforms over time. Number of electrodes with good or fair signal is plotted on the y axis against time in days after initial recording session (41, 28, and 1 day after implantation of electrodes) on the x axis for the three monkeys DE, RN, and CL. x-axis is on a logarithmic scale with the "1 year" mark shown with an arrow. Note the extended time period for monkey RN and the early frequent surveillance in CL.

B. Quality of Signals

Waveforms were evident on the majority of electrodes for the 569, 179, and 83 days after implantation for which the signals were evaluated, although there were day to day fluctuations in the number of electrodes providing identifiable waveforms. The reliability of obtaining signals was evaluated qualitatively by

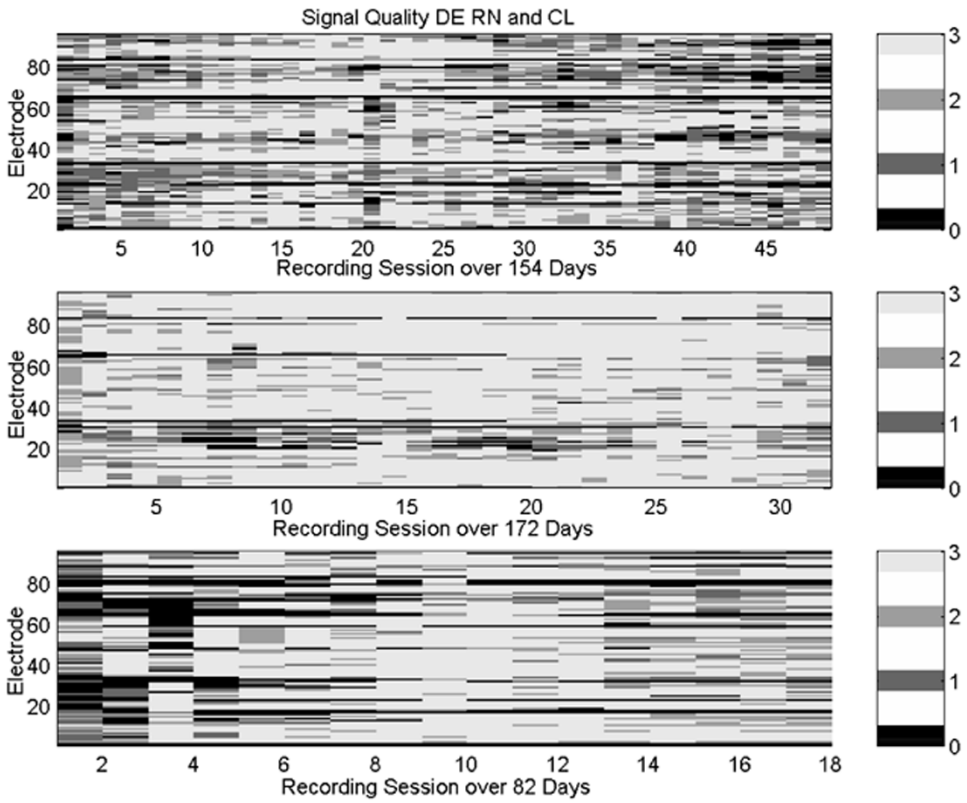

Fig. 10. Signal quality over recording sessions. Changes in signal quality (defined in the text) over recording sessions are plotted in this figure for each of the study monkeys DE, RN, and CL. For each subplot, the x axis represents the recording session, the y axis each electrode on the array, and the grey-scale value shows the signal quality corresponding to the grey-scale legend on the right.

plotting either the number or quality of waveforms for each electrode over time. The number of electrodes with signals rated as *good* or *fair* for each of the testing sessions for each monkey is shown in Fig. 9. Quality of these signals by the rank scale is illustrated in Fig. 10 in which signal quality is shown across multiple sample periods (separation between data points are 2.9 ± 2.7 (mean $\pm$ standard deviation), range 1–14 days, median 2 days; 5.5 ± 11.1, range 1–63 days, median 3 days; and 4.8 ± 4.8, range 1–15 days, median 3 days for DE, RN, and CL, respectively). This graph shows that overall signal quality remained relatively high and stable throughout the duration of recording sessions in each of the three monkeys. However, signal quality can vary on a particular channel between sessions. Note that signals can appear on channels that have had poor recordings across many sample sessions, as denoted by a black horizontal line becoming white or gray, and that signals can become poor (or lost) on channels that have been successfully recording as noted by reverse examples in the grayscale coding. Nevertheless, there is no overall noticeable trend evident in either the number of channels or their quality, as seen in Figs. 9 and 10.

To begin to address the early time course of recording reliability, recording sessions were conducted consecutively for five days, starting 23 h after insertion of the array in one monkey (CL). The signal quality as well as the number of active channels improved over the first five days after implantation in this monkey (Figs. 9 and 10, lower graph). A similar trend may have occurred in DE which was measured in the second week of recording. By contrast the one early sample in monkey RN is not consistent with this view. Other factors may be contributing to differences in early reliability. Overall, these data indicate that electrode yield is most variable during the initial 6–10 weeks after implantation (Fig. 9), but that greater than 50 waveforms can be reliably detected within two weeks after implantation. The evaluation of the array implanted in monkey RN was extended to 569 days after implantation. Even after 1.5 years after array placement, 76 electrodes still provided good or fair waveforms (Fig. 9).

C. SNR Over Recording Sessions

SNR provides a quantitative measure of reliability. SNR was calculated for waveforms on each electrode for randomly selected sessions for the three monkeys during a period of 143, 61, and 210 days after implantation for DE, CL, and RN (8, 11, and 18 sessions), respectively. The sampling of sessions for this analysis were throughout the entire recording period for DE and CL but only covered the first half of recording time-frame for RN. As suggested by qualitative scores, there were individual fluctuations in SNR. However, there was no statistical trend of diminishing SNR over the time period (Figs. 11 and 12). Furthermore, there was no significant change in mean SNR between first and last day of recording in the three monkeys (t test with Bonferroni correction $p = 0.681$, 95% confidence interval -0.419–0.640) (Fig. 12). In two monkeys (DE and CL), the SNR improved after the first four recording sessions for some electrodes (Fig. 11, first and third graphs). In support of a valid relationship between SNR and subjective signal quality, the two

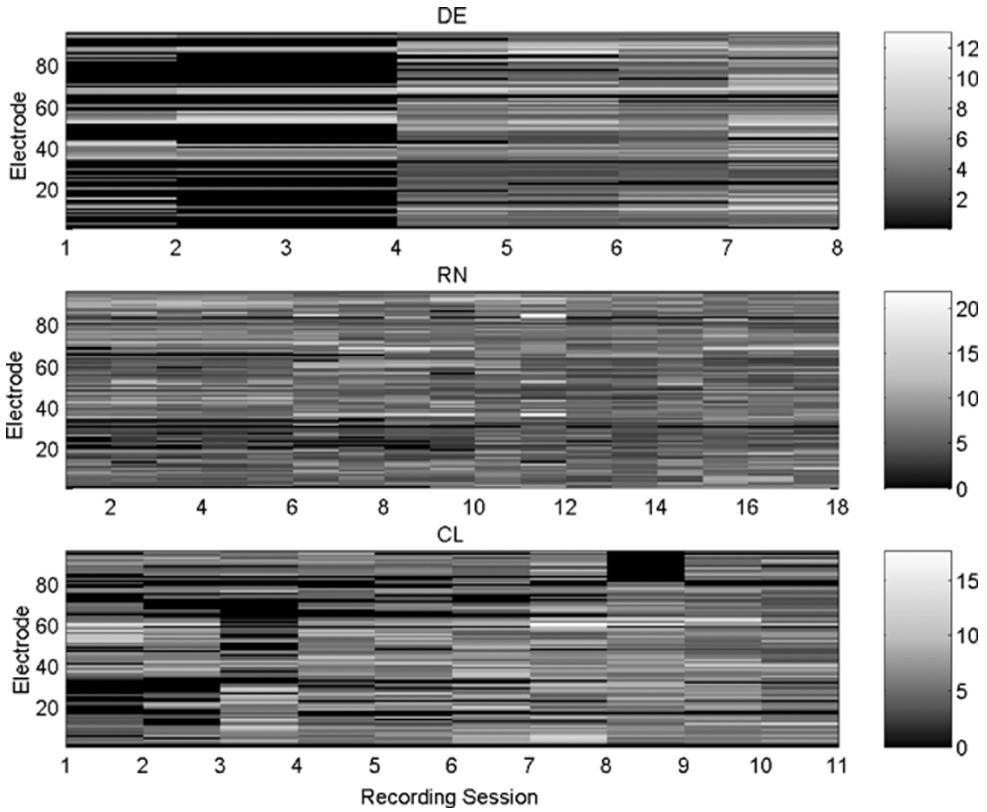

Fig. 11. SNR over recording sessions spanning 61–210 days. Changes in SNR over recording sessions are plotted in this figure for each of the study monkeys DE, RN, and CL. For each subplot, the x axis represents the recording session, the y axis each electrode on the array, and the grey-scale shows SNR corresponding to the legend on the right.

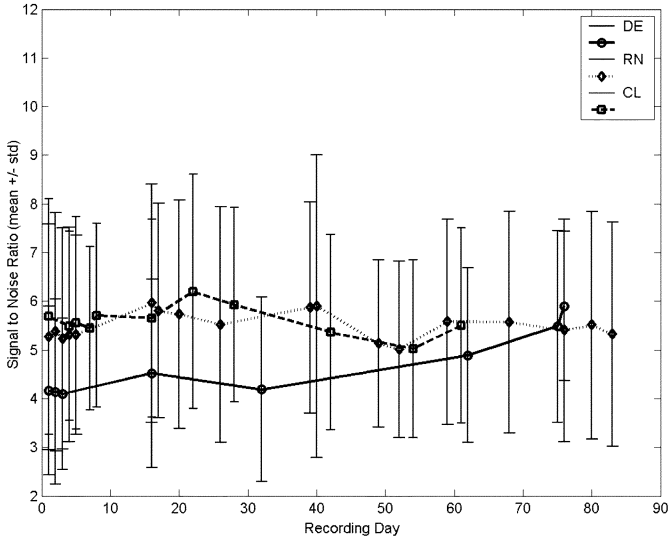

Fig. 12. Mean SNR over time. Mean SNR of signals obtained from all of the electrodes over recording sessions for three monkeys are plotted in this graph. x axis represents recording day starting with the first recording session (77, 127, and 1 days after implantation for DE, RN, and CL, respectively) and the y axis mean SNR. Error bars denote standard deviation. Different lines denote the three study monkeys (solid: DE, dotted: RN and dashed: CL).

variables were significantly correlated ($r = 0.71$, $p = 0$; 95% confidence interval 0.60–0.80). SNR analysis also confirmed that useful recordings could be obtained for the duration of the testing periods.

D. Array SNR Distribution Over Time

The distribution of SNRs also appeared to be stable across sample intervals. Histograms showing the SNR distribution are plotted for all of the units from all electrodes in the three monkeys (Fig. 13). The most prevalent SNR was between 3 and 4 and there was no pattern of diminishing trends in the distribution of this SNR as a function of time, which would suggest a decline in recording reliability. Thus, the range of observed SNRs was consistent across recording sessions.

E. Same-Day Variation in Signals

Large variations in signal amplitude within a day would result in unreliable recording. Amplitude variations during recording could result from electrode movement with respect to neurons either from mechanical forces on the array or due to respiratory and cardiac cycle induced movement of the brain. We evaluated the peak-to-peak amplitude of action potentials of 69 units recorded from 32 electrodes for two separate recording sessions in two monkeys over 35–53 min of continuous recording with the animal performing an arm movement task [Fig. 14(a)]. Slopes of a linear fit through the points were calculated for each unit depicting the rate of change. There was a distribution of slopes ranging from -0.1 to 0.2 with the majority around zero, indicating that neuron recordings were stable and showed no overall trend during the recording session [Fig. 14(b)]. Variation in noise amplitude was not analyzed.

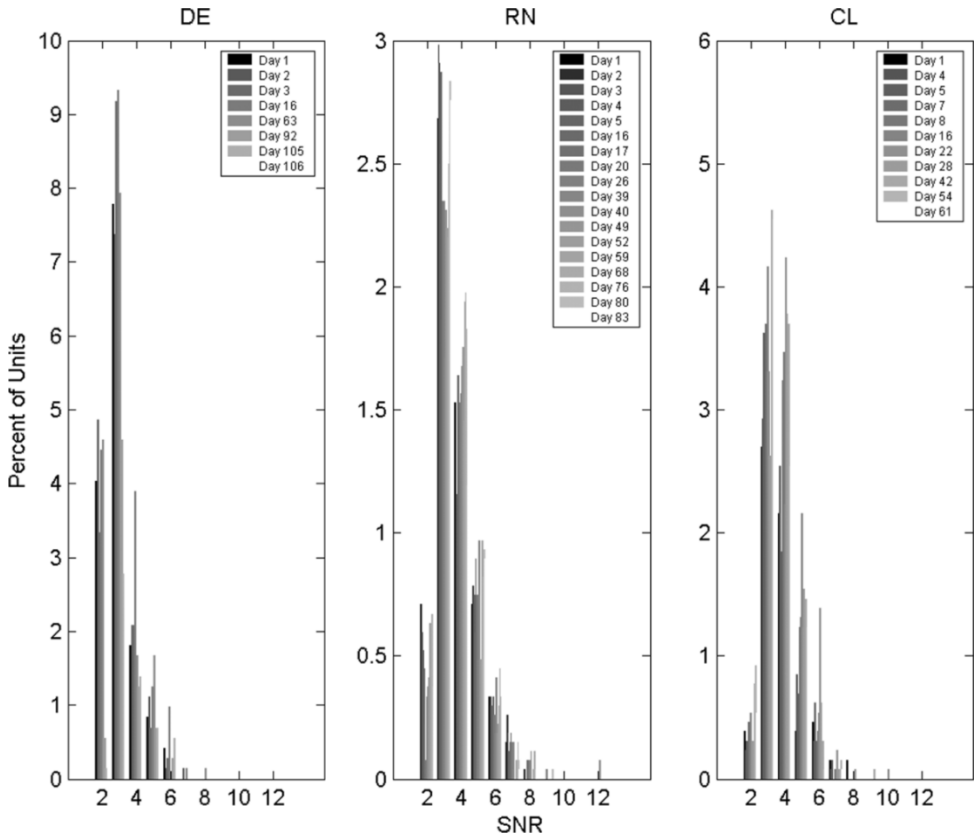

Fig. 13. Distribution of signal to noise over recording sessions. These series of bar graphs display the distribution of SNRs over recording sessions for three monkeys (DE, RN, and CL, respectively, from left to right). For each bar graph, the x axis represents SNR and the y axis is the percentage of units. Different grey-scale bars correspond to recording session times (from dark depicting earlier to light indicating later recording sessions as displayed in the legend for each graph).

F. Waveform and Activity Patterns Over Time

A reliable sensor would ideally provide recordings from the same set neurons for extended times. Stable waveform shape and firing patterns would be consistent with this requirement. We evaluated the reliability of these features across recording sessions using action potential shape and inter-spike interval. Due to the high-dimensionality of these features and the absence of knowledge about their true distributions, we did not utilize an absolute measure of reliability. Instead we employed relative measures which quantify the degree to which the wave shape and ISI distribution change over time for each electrode. Shape was defined using principal component decomposition and changes in these shapes were quantified by plotting the standardized distance between principal component cluster centers. For a given electrode and across all recording days for a given animal, the standardized distance between the center of the principal component cluster of a reference unit and the center of each other cluster is plotted as a function of time separation between recording sessions (see Methods). Unstable recordings would appear as an increase in the mean and variance of this measure over time. However, as shown in Fig. 15, this trend did not emerge. A similar analysis for ISI separation was also not significantly correlated with time between recording sessions separated by up to 91 days (Fig. 15). The PC and ISI distances were significantly correlated ($r = 0.16$; $p = 0$).

G. Electrode Impedance

Degradation in recording capabilities over time could be expected to emerge through reactions at the electrode–tissue interfaces, such as gliosis or electrode degradation, which could be reflected by a change in electrode impedance over time. To test this hypothesis, impedances were measured periodically in two animals, with a range of 1 day to several months between measurements. In order to identify a relationship between electrode impedance and signal quality, impedance and SNR were plotted graphically. Signals with high SNR were recorded from electrodes with a wide range of impedances from 50 $\mathrm{k}\Omega$ to over 1 $\mathrm{M}\Omega$ (Fig. 16) implying that there is no "ideal" electrode impedance for recording. Impedance ranges differed across the animals. For monkey RN, with post-implant, *in vivo*, electrode impedance of $189\ \mathrm{k}\Omega \pm 16\ \mathrm{k}\Omega$ (range: 50 $\mathrm{k}\Omega$–900 $\mathrm{k}\Omega$; median 170 $\mathrm{k}\Omega$), impedance and SNR were significantly correlated ($r = 0.2$; $p = 0$). For monkey CL, with post-implant electrode impedance of $612\ \mathrm{k}\Omega \pm 101\ \mathrm{k}\Omega$ (range: 40 $\mathrm{k}\Omega$–1000 $\mathrm{k}\Omega$; median 638 $\mathrm{k}\Omega$), there was no significant correlation between impedance and SNR ($r = 0.09$; $p = 0.06$). Overall, combining data from both monkeys, SNR and electrode impedance were not correlated ($r = 0.0012, p = 0.97$) (Fig. 16). However, both individually and when grouped, CL and RN impedances correlated well with signal quality ($r = 0.18$, $p = 0$; confidence intervals: 0.13–0.22). This suggests a loose association between impedance and the signal quality in the impedance range typi-

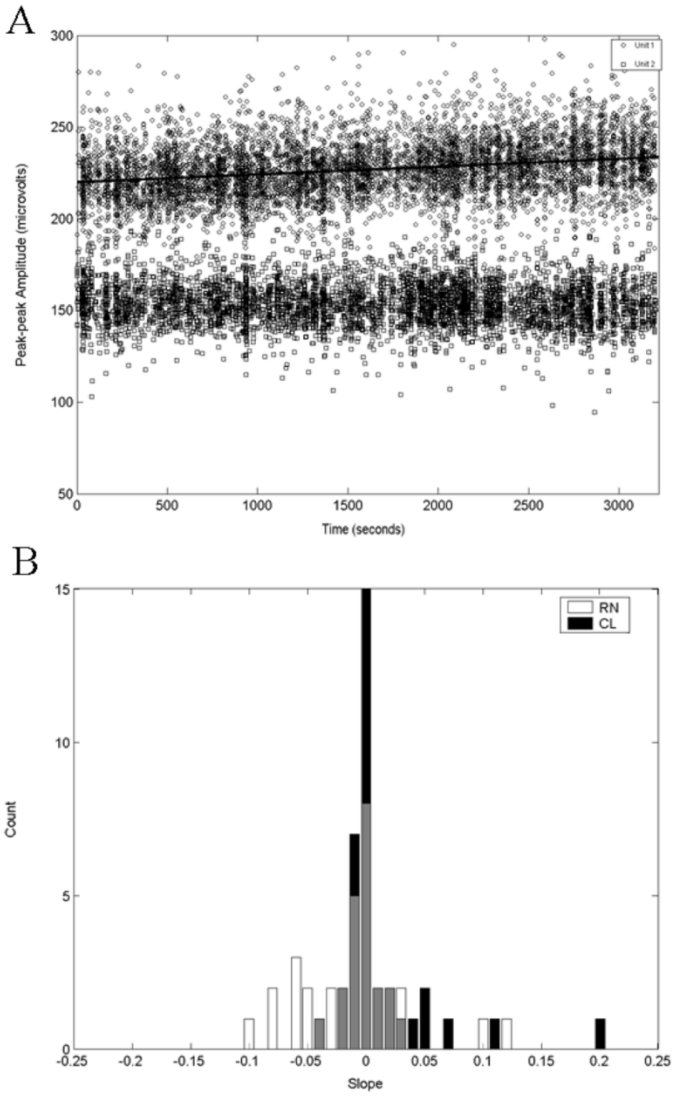

Fig. 14. Peak-to-peak amplitude changes over same-day recording sessions. (A) Peak-to-peak amplitude of two separate waveforms from one electrode (electrode 77 in CL) in one monkey is plotted as a function of time over a 53-min recording session. x axis depicts time in seconds and the y axis peak to peak amplitude in microvolts. Circles represent peak-to-peak amplitude of one waveform, whereas the squares show a different waveform from a single electrode. Black line represents a linear fit (slope: 0.0042 for unit 1 and $-0.000\,86$ for unit 2 (no line shown for unit 2)). (B) Distribution of slopes from two monkeys is shown in this graph. Black bars represent the slopes from monkey CL and the white bars from RN. Overlapping bars are shown in grey.

cally observed with the Bionic array. Impedance measurements in the brain fluctuated approximately 30% from day to day for most electrodes. In order to ascertain a temporal pattern of electrode impedance fluctuation, the ratio of impedances measured at later times to those measured at earlier times after implantation were compared for two monkeys (over an 83-day period). In RN, there was no statistical difference in the impedance ratios (mean ratio 1.01 ± 0.31; range 0.49–2.4; $p = 0.09$ with confidence intervals -1.74–1.92). In CL, however, the difference in early versus late impedance was statistically significant (mean ratio 1.23 ± 0.39; range: 0.5–3.5; $p = 0.0013$ with confidence intervals -12.4–3.7) suggesting an increase in impedance over time. However, SNR and signal quality did not diminish over the same intervening time period in either monkey.

H. Reliability of Movement-Related Signal

The motor cortex is characterized by neurons that modulate their discharge rate with movement. Arm area neurons are often tuned to the direction of reach, so that they fire maximally in a preferred direction (PD) and fire less as directions deviate from the PD. The ability to continually detect neurons carrying movement related activity is an essential requirement for neuromotor prosthesis sensors. The similarity of properties of neurons randomly encountered using the array compared to those selected by single, moveable microelectrodes is one measure of the value of the electrode array as a research tool. Movement-related modulation of neural activity was readily encountered on many of the simultaneously recorded neurons. Fig. 17 shows raster and histogram plots for all of the sorted waveforms recorded from an array in M1 during one session (RN 3-24-2003; 160 sorted units; movement direction to the "left," 180°) while the monkey performed an eight direction push-button task. Note that cells that modulate with movement onset (time after cue to move at 0 on time base) are very common. Fig. 18 illustrates one (RN 03-24-2003, electrode 42a) prototypical directionally tuned unit.

I. Direction Tuning of Units

Decoding of intended direction is dependent on direction tuning. In particular, it is necessary to have a broad distribution of tuning directions represented in the cohort of neurons sampled by the sensor for optimal decoding. We evaluated the occurrence of directionally tuned neurons and found that a wide-ranging distribution of directionally tuned cells is reliably present on the array. Preferred movement directions were calculated for all of the units sorted from the signals obtained from the array during different recording sessions. Overall, 66% of all units displayed a preferred direction (see Methods). While the preferred direction distribution could vary from day to day, the distribution of the mean preferred directions was even across 360° over 83 days (ANOVA $p = 0.102$) (Fig. 19).

J. Results From Earlier Versions of the Bionic Array

Data from three additional monkeys (TM, CO, and BD) not selected for detailed analysis, were retrospectively selected to compare with findings presented here. Recordings for these three monkeys were made over 870, 425, and 92 days, respectively. The arrays used in these studies were earlier versions of the Bionic array with certain differences in manufacturing and materials used. In particular, earlier electrodes had silicone nitride insulation that has since been replaced with parylene. A second change is that cables were soldered to the original arrays and are now wire bonded. Otherwise, these arrays were the same silicon probes with Pt tips as found in the current version of the sensor. Qualitatively, Si nitride coated arrays appeared to have much poorer SNR than the current sensor, perhaps due to a lower dielectric constant of the silicon nitride coating used, compared to parylene. Consistent with this view, the yield from each "early" array varied from 10% to 85% of the electrodes with a mean of $\sim 40\%$ (representing a maximum

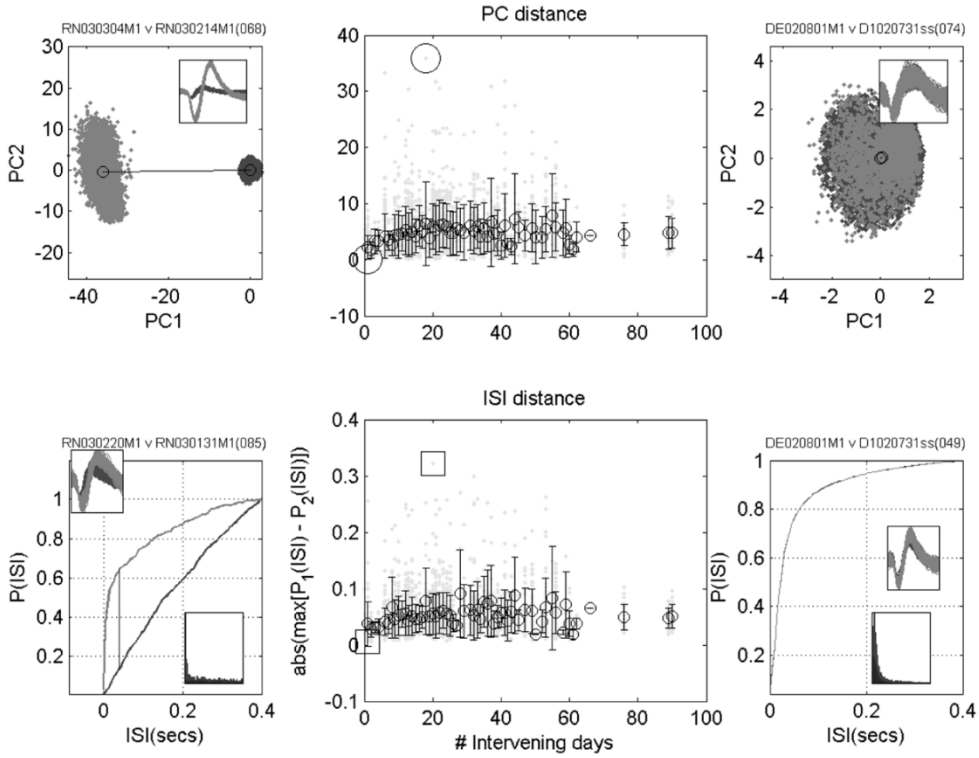

Fig. 15. Waveform and neuronal activity differences over time. Center top graph shows the standardized distance between the center of a cluster defined by waveform principal components (PC 1–4) of a reference unit and the cluster center for each comparison unit (see Methods), on the y axis, plotted against the number of intervening days between recordings on the, x axis, for all electrodes with > 200 waveforms and $\mathrm{SNR} > 3.0$. Light grey dots denote the individual distances, the black circles their mean, and the error bars, standard deviation. Graphs on the right and left show examples of the analysis performed on the data points (in center graph) corresponding to the smallest and largest distance, respectively (enclosed by large circles in the center graph). These graphs show the clusters in PC space. Standardized distance between the center of dark grey cluster to light grey cluster center is shown with a black line. First 200 waveforms of the units are plotted in the inset. Colors correspond to the PC clusters on different recording sessions, i.e., dark grey waveforms correspond to the dark grey cluster. Distances are normalized by the dark grey cluster standard deviation. Bottom graphs have the same layout. Center bottom graph shows the distances between ISI cumulative distribution curves for each unit selected, as above. Side graphs show the ISI in seconds plotted against P(ISI) (corresponding data points are enclosed in large squares in the center figure). Inserts show the waveforms and ISI histograms in matching shades of grey.

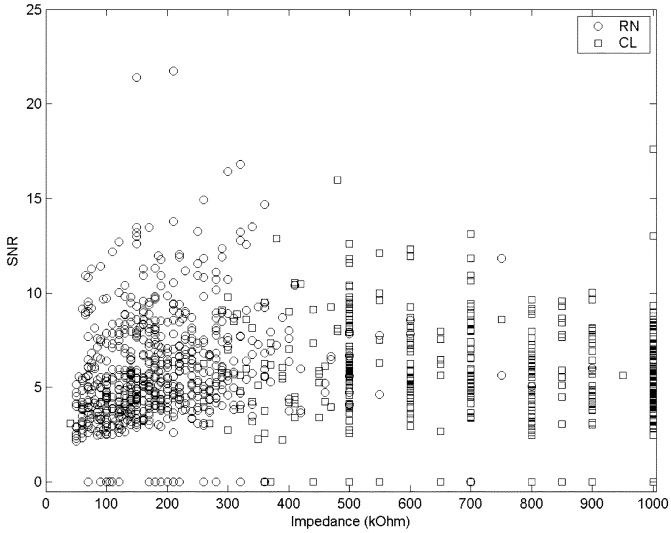

Fig. 16. Correlation of impedance and SNR. Impedance along the x axis (in the range 0–1 $\mathrm{M}\Omega$) is plotted against SNR along the y axis in this graph. Circles are data from monkey RN and squares from CL.

of 32 sorted units from 47 electrodes). Individual electrode impedances in the earlier arrays, initially ranged from 50 to 600 $\mathrm{k}\Omega$. There was no correlation between signal quality and initial electrode impedance for these arrays. Despite differences, these additional data confirm the ability to obtain long-term recordings with these silicon multielectrode arrays.

K. Recording From Parietal Cortex

Signals useful for the control of neural prostheses may be desired from other areas of the cortex. Parietal cortex is one of several cortical areas which contain movement related neurons that could be a source of outputs. Most other cortical areas have smaller neurons that may make recording with the Bionic sensor less reliable. We tested the ability to record signals in parietal cortex in three separate monkeys (LV, SP, and RD) each consecutively implanted with Bionic arrays, in area 5D of parietal cortex, located midway between the interparietal sulcus and a dimple evident medially on the postcentral gyrus. Waveforms comparable to signals obtained from M1 described in this paper were obtained from these animals, although there was a subjective impression that fewer neurons were recorded. However, the SNR, action potential waveforms and signal quality were generally similar to signals obtained from M1 (Fig. 20), indicating that recordings are possible from this area.

L. Recording Failure and Array Replacement

A total of 36 implants in 16 other monkeys, which were not systematically evaluated for reliability here, provided successful

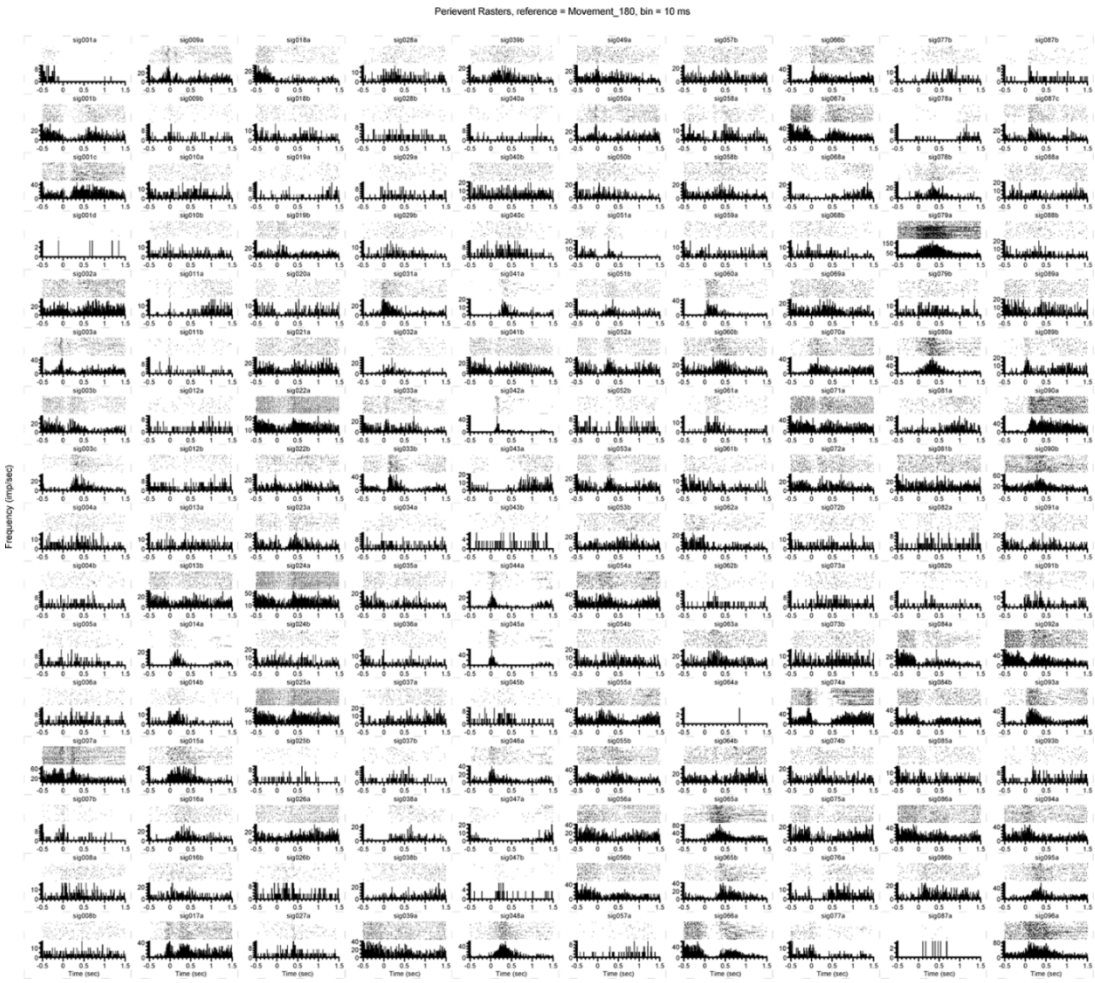

Fig. 17. Raster and histogram plots of sorted waveforms recorded during one session illustrating the prevalence movement-related modulation. Each plot represents a unit recorded from one electrode. Multiple units from a single electrode were recorded (160 units from 96 electrodes). Each x axis represents -500 to 1500 ms range. Time 0 represents movement onset. Each y axis depicts cell firing rate (spikes/s).

recordings for up to 1264 days. This group was implanted using different array coating materials, connectors, and surgical procedures that were part of the longitudinal development of the system studied here. Of this latter group, recordings in the majority $(n = 12)$ were ended because of observed motion or separation of a methacrylate acrylic cap, used to secure the appliances, from the skull or from mechanical failure of the connector. Recordings in two of the earliest monkeys were ended for reasons attributed to surgical procedures and one related to a meningeal infection that appeared to have spread intracranially from below the acrylic through a screw hole that secured a head restraint post. Removal of acrylic from the implant surgical procedure is designed to eliminate this source of unreliability in the system. In earlier studies, in two of three monkeys, arrays were removed. In both cases, arrays and connectors had been secured with acrylic cement applied over the skull. Loosening of acrylic required removal of the cap and sensor at 92 and 425 days (BD and CO, respectively) after implantation and subsequent aldehyde perfusion for histological investigation after euthanizing the animals. The use of acrylic cements to secure the assembly is no longer used.

In the current study, recordings failed acutely in DE 468 days after array implantation immediately after an acrylic skull cap was placed during a surgical procedure to stabilize a pedestal which had loosened on the head. It is assumed, but not verified, that the wire bundle to the connector was damaged during this procedure. Recording failure was evident in CL two months after implantation as a result of the animal severing an exposed area of the wire bundle. We remained able to record good signals from RN at the time of data analysis for this paper at 640 days after implantation of the array.

In three instances (LV, CL, and RN), replacement arrays were implanted, in the same spot of motor cortex, after removal of original arrays. Neural signals similar to those presented in the results of this paper were recorded from all of these arrays indicating a lack of local injury to the cortical tissue. The data obtained from monkey RN, presented here, was obtained from the third array implanted in the same location of M1 after removal of previously placed arrays (Figs. 5 and 9). This array was implanted approximately on top of the original insertion site. These data indicate that arrays can be replaced and the replacements can function reliably. These data also show that there is no large

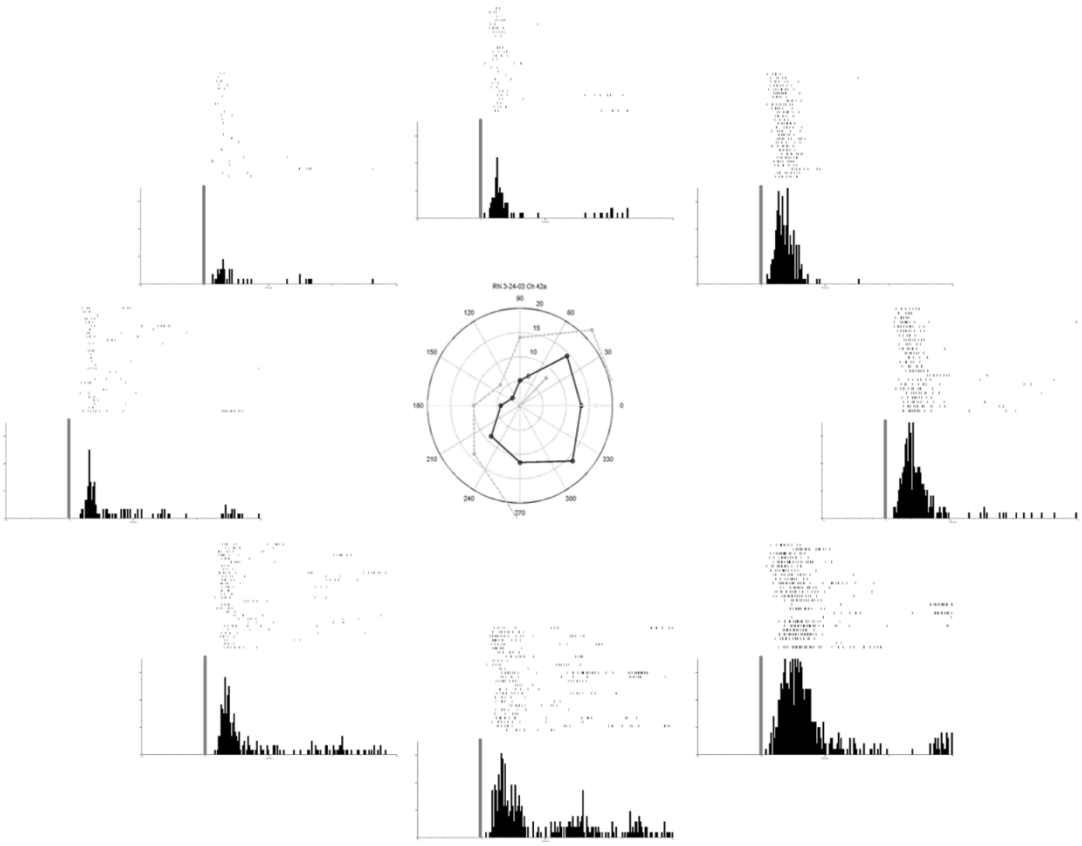

Fig. 18. Representative example of the direction tuning properties of one unit recorded during one session. Plots along the circumference show raster-histograms of the firing rate for the unit. Vertical line shows onset of movement. Axes are as in Fig. 15. Center figure shows the maximum and mean firing rates (bold and light lines, respectively). Preferred direction is calculated as 0° in polar coordinates for this example (with 0° to the right and advancing counter-clockwise).

scale damage that would interfere with replacement of an array and subsequent recording of good quality signals from the new array.

IV. Discussion

A detailed prospective analysis of chronic implants in three monkeys evaluated the reliability of the Bionic implantable microelectrode system to record multiple neuronal spiking activity from the primate MI cortex. The evaluation tested not only the 100-microelectrode array, but also the cabling between the surface of the brain to the cranium and a high density percutaneous connector necessary to gain access to the sensor's signals. The results show that neural waveforms may be obtained at any time from the majority of the electrodes in three monkeys for at least three months after insertion and in one monkey for more than 1.5 years. Additionally, recordings for more than one year have also been reliably obtained in nine other monkeys studied on our laboratory, but not part of this prospective evaluation. The system remains reliable over this time, based on the lack of any systematic change in signal quality, SNR, impedance, or the range and variation of waveform shape. Further, the electrodes reliably detect neurons carrying movement-related information in MI and are able to detect neural activity in other cortical areas. These data combined with our earlier series of 36 less fully evaluated implants in 16 additional monkeys indicate this system should be able to provide signals for years. However, we cannot predict what could happen to the signals past the evaluation period because of the complex biological milieu which interacts with the electrodes. These findings further indicate that planar arrays of silicon-based microelectrodes employing a standard microelectrode architecture can be useful research tools and valuable sensors for neuromotor prostheses.

A. Microelectrode System

The details of the design and fabrication of the microelectrodes have been described in detail elsewhere by Normann and colleagues [4], [6]. It is worth noting a few fundamental differences in the design of this system and others now being tested for purposes of discussion. The Bionic array consists of a regularly spaced set of microelectrodes each of which is tapered to a point. This geometry mimics that of traditional sharpened metal or glass electrodes that have been successfully used for decades during acute single neuron recording. Taper and the point may be important during insertion to minimize damage [10]. The array is inserted rapidly, which creates some damage as the tip drives through the cortex, but our data shows that this damage does not prevent reliable long term recording. The Bionic Array has a planar support platform that rests upon on the cortical surface, which may add stability necessary for long term reliability. Microwire arrays are also used as a chronic recording electrodes. These consist of bundles of ~ 50 μm metal wires, typically glued together and cut off into blunt tips, which serve as the recording sites, before insertion. They are typically inserted slowly taking 8–10 h which may help to reduce damage

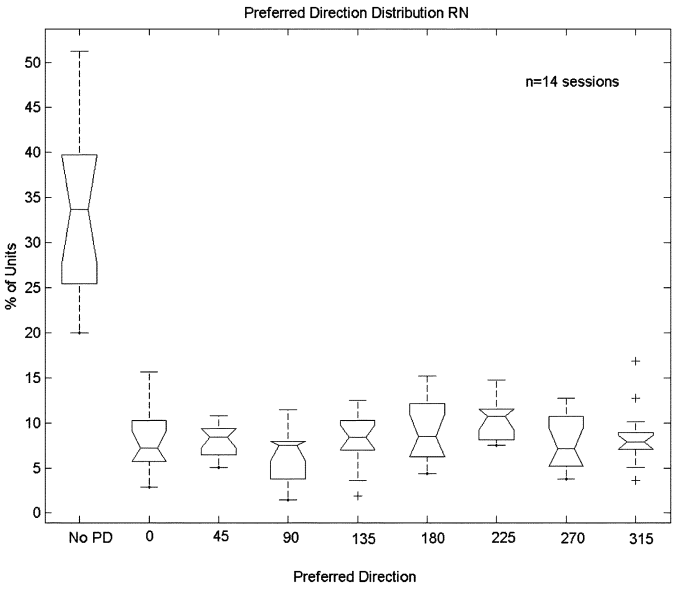

Fig. 19. Distribution of preferred directions for all recorded units. This box and whiskers plot shows the distribution of the preferred directions of all the units recorded during 14 sessions from one monkey RN. Individual box and whiskers plots represent the preferred directions as labeled on the x axis. First plot shows units with statistically similar firing rates in all directions (No PD) and the next eight plots show preferred directions 0° through 315°. y axis shows the percentage of units. Box has lines at the lower quartile, median, and upper quartile values. Whiskers are lines extending from each end of the box to show the extent of the rest of the data. Outliers are data with values beyond the ends of the whiskers. Notches represent a robust estimate of the uncertainty about the medians for box to box comparison.

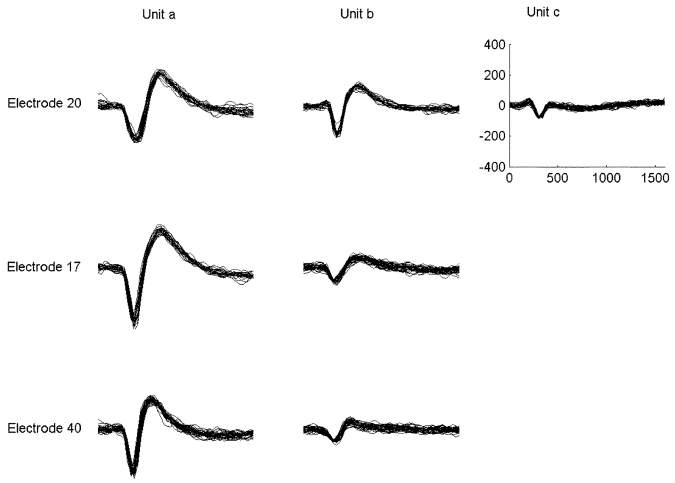

Fig. 20. Representative example of waveform shapes from array in area 5D. Seven sorted units (each waveform shape shows 50 superimposed classified signals) on three separate electrodes during a recording session from one monkey (SP) are shown in this figure. Each unit is designated by a column and is labeled at the top (unit a–c). Each separate electrode is displayed in a row and is labeled on the left (electrode 20, 17, and 40). Scale indicated on the top right waveform (x-axis, time: 0–600 μs; y-axis, amplitude: -400–400 μv) applies to all waveforms in this figure.

from blunt tips [11]. A third technology, generally know as Michigan electrodes, consist of single or multiple flat probes of silicon with multiple, photolithographically placed recording patches along the length of each. Currently, the pointed probes are pushed by hand into the cortex [11]. Microwires are affixed to the skull, which makes them more likely to move with respect to the brain, compared to the Bionic array electrode which is designed to float with motion in the brain. Motion of the brain could continually damage the brain and decrease reliability. Although not documented here, we typically see a well developed capsule over the back of the array that firmly anchors the array to the cortical surface. This may help the array float and dampen possible tethering forces. Bionic and Michigan electrodes have a strong advantage of being fabricated by controlled processes with defined geometries so that reliability issues across animals can not be attributed to differences between sensors. However, Michigan electrodes arranged into a dense planar array are only in prototype form and have not been tested as chronic implants in primates [12]. Bionic electrodes (and often microwires) have the disadvantage of having all electrodes at a single depth, which can limit recording to the cells at the available depth, while Michigan electrodes allow sampling from a vertically aligned set of sites. Finally, the materials used in the three systems may affect reliability. Only known biocompatible and biostable materials-Pt, parylene, and silcone, contact tissue for the Bionic array. The system has passed animal toxicological screening [13]. Tissue contact for microwires includes a variety of materials, depending on investigator, but epoxies and Teflon are common, as well as tungsten or stainless steel. Michigan electrodes also include silicon nitride coatings. The biocompatibility and biostability of silicon has been extensively investigated histologically [14], [15]. Dental acrylic is typically used to secure both microwires and the Michigan electrodes to the skull without contacting the brain surface; it does not present a concern to the neural interface, but is a foreign material that could be source of infection or implant rejection, as found in our implants.

B. Number of Neurons

One goal of multielectrode recordings is to obtain signals from the largest possible number of neurons at the same time. The Bionic array provided signals on a majority of available electrodes. A mean of 120 waveforms could be extracted from the 96 available electrodes with more than 99 waveforms (76 channels $\times$ 1.3 units per channel) classified qualitatively as "good" to "fair." Whether these waveforms represent single units or mixtures of units, is often difficult to verify because there is no established standard method of sorting waveforms. Clearly units ranged from very well isolated with $\mathrm{SNR} > 20$, to poor, which likely represent mixtures of neurons. Many waveforms classified as good/fair had distinctive features, suggesting that a substantial percentage may be single neurons. Methods to verify single units from among mixtures of waveforms are still under development and there may be applications in which both well-classified and poorly classified neurons may provide useful information. For example, a neuromotor prosthesis may be as effective with multiple as with single units [1], [16]. Thus, classification standards will need to be established in order to make definitive statements concerning the total number of single neurons. The yield of useful waveforms may be higher in MI than other areas because MI neurons contains larger neurons than found in other cortical areas. However, recordings obtained from both parietal and premotor areas, suggests that the array can provide signals from many cortical areas [17].

Another factor that may affect the number of waveforms detected is electrode impedance, although this remains a complex measure of recording efficacy. Detecting waveforms is a function of the geometry and surface area of the exposed recording surface, as well as the materials used to record. Impedance is related to these features, but not in a clearly established manner-impedance is a function of the electrode material, tip plating, and insulating materials used. The electrodes tested here have relatively low impedances, in the range of 50–800 $\mathrm{k}\Omega$ compared to those typically used in single microelectrode recordings, which are often in the low megaohm range. Tip impedances in the present study did not show a systematic relationship to recording quality; we had just as many recorded waveforms on the array that had systematically higher impedances as for the lower impedance arrays (612 $\mathrm{k}\Omega$ versus 189 $\mathrm{k}\Omega$). Relating tip impedance to waveform isolation may be confounded by the proximity of the electrode to a cell, cell packing density, glial response at each electrode, and other factors. We can only conclude that the range of impedances used in this study reliably provides signals. In this study, simple impedance measurements were recorded. Other investigators have used more sophisticated methods including impedance spectroscopy to determine electrode impedance which may reveal correlations with recording variability that are consistant with encapsulation [18]. Glial reaction is a known consequence of inserting foreign material into the nervous system [10], [19]–[25]. However, we find that glial response does not materially affect the recordings we are making, at least for the 1.5 years measured here. The biological environment is dynamic, so we cannot predict what responses might occur with longer implant times so that gliosis, infection, material degradation, or mechanical wear may cause the implant to fail. Other investigators believe that, of these responses, gliosis is the most likely to affect the long-term viability of the recorded signals and are devising techniques to minimize reactive cell and tissue responses to chronically implanted electrodes [20], [22].

C. Stability and Longevity of Signals

An ideal array would record high quality signals from the same set of cells indefinitely. In our study, recordings were reliably obtained across the duration of our analysis (up to 569 days) on the basis of both the number waveforms and quality of the signal obtained. The observations here were limited to 61–569 days. However, earlier arrays not evaluated systematically in the present study recorded signals for more than three years. Three measures showed that the overall system remained stable across this period: SNR, impedance, and the range and variation of waveforms.

SNR was measured for a randomly selected sub-sample of recording times. There was no change in SNR across these time periods in three monkeys. Early variations were seen in signal quality and SNR. These findings are consistent with other studies [26]. Our data revealed that time between recording sessions and waveform characteristics were not correlated. An association would be expected if signals were adversely influenced by biological factors such as gliosis at the electrode tip or neuronal death from disruption of vasculature during electrode insertion. Investigators in other studies have documented vascular damage using Perl's Prussian Blue reaction and local inflammatory responses with glial fibrillary acidic protein (GFAP) staining, after array insertion and following a period of stabilization over several weeks [14], [15]. However, these factors are unlikely to influence signal characteristics over the long term unless they continue, which remains a strong possibility in dynamic biological environments like the brain. It is nearly certain that the insertion of the electrode array in our experiments, as would any object inserted into the brain, resulted in disruption of at least capillary sized blood vessels. The cortical capillary bed is densely packed, with spacing on the order of 40 μm in primate cortical tissue [27]. Fluctuations in the signal quality seen shortly after array implantation may be due to this initial direct damage and tissue reaction. Further, functional suppression of neurons and alteration of neuronal excitability from bioactive products released due to bleeding caused by the insertion process may contribute to variations in signal quality and SNR. Improvement of the signal quality and increased yield, for which there was no clear trend in the three animals, may result from recovery produced by variations in the intial insertion injury. The data presented demonstrate long-term good quality signals as well as directionally selective neuronal responses from the majority of electrodes, which is strong evidence for the lack of long-term neuronal injury from insertion effects.

A second measure of stability in the array is impedance. A rationale for measuring impedance is to detect overgrowth of tissue that isolates the electrode, which should be reflected as an increase in impedance and a correlated decrease in signal quality. Impedance changes over time were variable in two monkeys; however, the signal quality and SNR of the population recorded by the Bionic array did not degraded over time, in support of this measure. In a separate study, flat silicon probes of the "Michigan" design in rats showed a doubling of impedance over a 45-week period, but recording yield remained at 90% [28]. Further, Schmidt *et al.* reported that impedance could vary threefold over a five month period, but this did not seem to affect recording quality [29]. This suggests that impedance is a poor measure of reliability except in cases of gross failure of the device where impedance may approach zero (shorting) or infinity (broken connection). The use of improved techniques for assessing impedance, such as impedance spectroscopy, may provide additional information related to glial encapsulation of electrode tips, but the value of this measure, in light of recording reliability is uncertain.

Waveform appearance is a third measure of reliability. This measure also remained stable across time. We found no correlation of the time between recording sessions and overall waveform characteristics (Fig. 15). On a shorter time scale, there was no systematic change in waveform amplitudes within sessions, suggesting high reliability of the population recorded at any one time (Fig. 14). These data indicated that, as a population, there is no systematic degradation in signal recording at least within the time frames examined here. While we found that signals were reliably recorded on the majority of electrodes for any session, we did not determine whether these were the same signals from

day to day. Marked changes in waveform were observed between days, but it is very difficult to evaluate what these changes mean. Waveforms for different neurons may be very similar and waveforms for the same neuron may vary dramatically in shape and polarity with changes in the relationship between the recording surface and the spike initiation zone. Prior studies of longevity of multielectrode systems have been performed in other species. Implanted microwire electrodes in monkeys can record for many months. Microwire arrays appear to have good yields initially, but reportedly diminish substantially in the number of recordable waveforms within 5–18 months or less, suggesting that they are less reliable as a long term device in primates [9]. Interestingly, recording longevity appears to be greater on smaller brained species such as rodents, where more than 80% of electrodes yielded signals starting at 2 weeks and up to 55 weeks after implantation, using either microwires or silicon probes [26], [28]. The reason for this species difference is not clear. However, a major concern has been the loss of signal over time due to glial scarring that isolates implanted sensors from neurons [10], [15]. Thus, it is possible that the greater longevity of arrays in rodents may be related to relatively less motion of smaller brains or to a species difference in glial responses. Our results favor the former interpretation: some of the other implanted technologies are fixed with respect to the skull allowing relative motion of the array with respect to the brain. By contrast, the planar substrate of the Bionic array sits on the cortical surface where it can move with the surface. The ability after more than one year to record signals similar to those seen weeks after implantation further suggests that glial responses are minimal, and, at least, inconsequential to recording for electrodes arrays of this design in primates.

D. Type of Information Available

Arrays implanted in MI readily recorded neurons that carried movement related information similar to those characterized using single, moveable microelectrodes. Neurons contained information about the onset of movement and its direction and these were cosine tuned to direction, as previously described [30]. These findings demonstrate that the neurons detected by the array are typical of motor cortex neurons and their characteristics suggest that they are functioning normally, at least by these measures. The results also demonstrate that neurons carrying directional information are reliably encountered in the majority (66%) of motor cortex neurons. Such information is critical for the design and operation of a neuromotor prosthesis and validates the use of these electrodes for study of movement encoding in motor cortex.

E. Failures

Failures can be beneficial in that they provide information for improved sensor systems. Failures can be classified as acute, due to abrupt changes (e.g., broken cabling) or evolving, potentially due to biological responses to the implant. In the present group, one failed following placement of an acrylic cap. No failures could be attributed to a biological response around the sensor, in that recording quality did not slowly degrade over time. This observation was similar in the group of 18 other monkeys studied during the development of the system. The main cause of failure was linked to the use of acrylic cement which often loosened, requiring the removal of the array. The acrylic skull cap often leads to bone remodeling causing softening of the platform where the connector is attached leading to mechanical instability of the connector and in some cases extra or (in one case) intracranial infection. In addition, failures across all of our animals studied resulted from ineffective connector prototypes, mechanical disruption of the cabling. These data will be systematically presented in a future publication. The elimination of dental cements and the creation of a high density, low insertion force connection mechanism helped to eliminate these issues.

The insertion of any material into the brain, including microelectrodes, is virtually certain to produce vascular damage, bleeding, and local inflammatory responses [14], [15]. Characterizing the form of this response and the amount of damage resulting is complex, and related to the nature of the materials used, the method of insertion, and the geometry of the array; effects may change over time as materials interact with a changing environment. We did not see failures that could be attributed to any of these features, suggesting that the form of these responses is acceptable for a chronic implant, although it will be valuable to continue to determine the nature of these effects at longer intervals. Interestingly there appeared to be the greatest variability in recording at the earliest times (Figs. 9–11), suggesting that either details of the insertion or individual differences in animals may influence recording.

F. Applications for Multielectrode Arrays

Reliable multielectrode arrays have a variety of scientific and biomedical applications. Simultaneous recordings of multiple neurons make it possible to evaluate the relationship of population activity patterns to behavior, cognition, perception, and sensory processing. Importantly, each neuron is recorded under identical experimental conditions providing a level of control for attention, motivation, and performance not possible with serial recordings. Multielectrode arrays will also allow for evaluation of neuronal timing relationships which have been thought to be related to certain higher level functions, such as visual "binding" [31]. Finally, chronic implants allow the study of changes in neuronal firing over time, as might occur with learning. However, reliable means to ascertain that the same neuron is recorded each day will have to be developed. Our work indicates that the population of recorded cells may shift from day to day. Multineuron recording systems are also potentially valuable to serve as sensors for new neurotechnologies. The recent demonstration that monkeys can use the decoded output of multiple neurons, including those recorded with the array tested here, as a control signal for goal directed behavior is a critical proof of concept toward the development of a neuromotor prosthesis (NMP) [1]–[3]. A NMP may be able to provide a new output source for paralyzed humans. The Bionic array has been approved by the FDA and now tested in one patient in a pilot study in quadriplegic humans; this study should provide valuable data concerning the ultimate design of a practical human NMP. Multielectrode arrays may also be valuable as a sensor in devices that detect abnormal neural firing patterns, alert patients to changes in brain state (as in epilepsy), or to control the delivery of therapeutic agents

including both drugs and electrical stimulation. The widespread need for ways to treat neurological and psychiatric diseases in humans is a strong motivation to continue to develop reliable neural activity sensors.

G. Limitations of the Bionic Array

The Bionic array has limitations that influence where it can be reliably used. The planar design of the Bionic array restricts its application to surface structures of the cortex and the current length availability of 1 or 1.5 mm further constrains what is accessible for recordings. However, it may be possible to design ways to insert the array in sulci and it is feasible to lengthen or shorten the electrodes. Microwires can be placed at any depth, although they require a tube to guide their trajectory into deep structures, which could produce greater damage than long, thin probes. Electrodes for the Bionic array are a single length, within a plane, so that they can not be targeted to multiple cortical layers and they are not adjustable once placed. Silicon probe electrodes allow for multiple recording sites on each electrode which can increase sample size and sampling across cortical layers; such multisite configurations are not currently available on the Bionic array. The reliability of recording a over long time and the steady proportion of movement related cells, suggests that the ability to continually reposition electrodes is not necessary for neural prosthesis applications. This may be very valuable for research applications. The array is also limited by having only 96 electrodes. Higher numbers may be desirable for a variety of reasons. However, there is no reason why multiple simultaneous arrays may not be implanted to increase yield. Preliminary data from four monkeys in our laboratory have demonstrated that multiple array implants are feasible.

V. Conclusion

We have demonstrated that it is feasible to record high quality, reliable signals from multiple electrodes, for periods of years after implantation using a silicon-based microelectrode array in motor cortex. This technology may be used to obtain control signals for prosthetic devices and for new research applications. The Bionic array has recently received investigational device exemption from the Food and Drug Administration (FDA) permitting investigators to explore human applications. Also, high quality, reliable, simultaneous recordings from multiple electrodes in M1of awake, behaving animals will facilitate improved understanding of the role and function of neuronal ensembles during the execution of movement. Finally, by using multiple arrays in different regions of the brain, investigators will have a useful additional tool to explore interactions between cortical neurons and cortical regions.

References

[1] M. D. Serruya *et al.*, "Instant neural control of a movement signal," *Nature*, vol. 416, pp. 141–142, 2002.

[2] D. M. Taylor, S. I. Tillary, and A. B. Schwartz, "Direct cortical control of 3-D neuroprosthetic devices," *Science*, vol. 296, pp. 1828–1832, 2002.

[3] J. M. Carmena, M. A. Lebedev, R. E. Crist, J. E. O'Doherty, D. M. Santucci, D. Dimitrov, P. G. Patil, C. S. Henriquez, and M. A. Nicolelis, "Learning to control a brain-machine interface for reaching and grasping by primates," *PLoS Biol.*, vol. 1, no. 2, pp. E42–E42, Nov. 2003.

[4] C. T. Nordhausen, E. M. Maynard, and R. A. Normann, "Single unit recording capabilities of a 100 microelectrode array," *Brain Res.*, vol. 726, pp. 129–140, 1996.

[5] A. Branner and R. A. Normann, "A multielectrode array for intrafascicular recording and stimulation in sciatic nerve of cats," *Brain Res. Bull.*, vol. 54, no. 4, pp. 293–306, Mar. 2000.

[6] E. M. Maynard, C. T. Nordhausen, and R. A. Normann, "The Utah intracortical electrode array: A recording structure for potential brain-computer interfaces," *Electroencephalogr. Clin. Neurophysiol.*, vol. 102, pp. 228–239, 1997.

[7] P. J. Rousche and R. A. Normann, "A method for pneumatically inserting an array of penetrating electrodes into cortical tissue," *Ann. Biomed. Eng.*, vol. 20, pp. 413–422, 1992.

[8] E. M. Maynard, E. Fernandez, and R. A. Normann, "A technique to prevent dural adhesions to chronically implanted microelectrode arrays," *J. Neurosci. Methods*, vol. 97, pp. 93–101, 2000.

[9] M. A. Nicolelis *et al.*, "Chronic, multisite, multielectrode recordings in macaque monkeys," *Proc. Nat. Acad. Sci.*, vol. 100, no. 19, pp. 11 041–11 046, 2003.

[10] D. J. Edell, V. V. Toi, V. M. McNeil, and L. D. Clark, "Factors influencing the biocompatibility of insertable silicon microshafts in cerebral cortex," *IEEE Trans. Biomed. Eng.*, vol. 39, no. 6, pp. 635–643, Jun. 1992.

[11] A. B. Schwartz, "Cortical neural prosthetics," *Annu. Rev. Neurosci.*, vol. 27, pp. 487–507, Jul. 2004.

[12] J. F. Hetke and D. J. Anderson, "Silicon microelectrodes for extracellular recording," in *Handbook of Neuroprosthetic Methods*, W. E. Finn and P. G. LoPresti, Eds. Boca Raton, FL: CRC, 2002, pp. 163–91.

[13] M. Serruya, private communication, May 2004.

[14] J. N. Turner, W. Shain, D. H. Szarowski, M. Andersen, S. Martins, M. Isaacson, and H. Craighead, "Cerebral astrocyte response to micromachined silicon implants," *Exp. Neurol.*, vol. 156, pp. 33–49, 1999.

[15] D. H. Szarowski, M. D. Andersen, S. Retterer, A. J. Spence, M. Isaacson, H. G. Craighead, J. N. Turner, and W. Shain, "Brain responses to micromachined silicon devices," *Brain Res.*, vol. 983, pp. 23–35, 2003.

[16] K. W. Horch and G. Dhillon, Eds., *Neuroprosthetics: Theory to Practice (Bioengineering and Biomedical Engineering S.)*, Singapore: World Scientific, 2002.

[17] N. G. Hatsapoulos, private communication, May 2004.

[18] J. C. Williams and D. R. Kipke, "Methods for modeling the relationship between extracellular recording variability and impedance properties of chronic neural implanys," in *Proc. 1st Joint BMES/EMBS Conf.*, vol. 1, 1999, pp. 486–486.

[19] P. M. George, A. W. Lyckman, D. A. La Van, A. Hegde, Y. Leung, R. Avasare, C. Testa, P. M. Alexander, R. Langer, and M. Sur, "Fabrication and biocompatibility of polypyrrole implants suitable for neural prosthetics," *Biomaterials*, vol. 26, no. 17, pp. 3511–9, Jun. 2005.

[20] S. T. Retterer, K. L. Smith, C. S. Bjornsson, K. B. Neeves, A. J. Spence, J. N. Turner, W. Shain, and M. S. Isaacson, "Model neural prostheses with integrated microfluidics: A potential intervention strategy for controlling reactive cell and tissue responses," *IEEE Trans. Biomed. Eng.*, vol. 51, no. 11, pp. 2063–73, Nov. 2004.

[21] J. Moss, T. Ryder, T. Z. Aziz, M. B. Graeber, and P. G. Bain, "Electron microscopy of tissue adherent to explanted electrodes in dystonia and Parkinson's disease," *Brain*, pt. 12, vol. 127, pp. 2755–63, Dec. 2004.

[22] W. Shain, L. Spataro, J. Dilgen, K. Haverstick, S. Retterer, M. Isaacson, M. Saltzman, and J. N. Turner, "Controlling cellular reactive responses around neural prosthetic devices using peripheral and local intervention strategies," *IEEE Trans. Neural Syst. Rehabil. Eng.*, vol. 11, no. 2, pp. 186–8, Jun. 2003.

[23] X. Cui, J. Wiler, M. Dzaman, R. A. Altschuler, and D. C. Martin, "In vivo studies of polypyrrole/peptide coated neural probes," *Biomaterials*, vol. 24, no. 5, pp. 777–87, Feb. 2003.

[24] X. Liu, D. B. McCreery, R. R. Carter, L. A. Bullara, T. G. Yuen, and W. F. Agnew, "Stability of the interface between neural tissue and chronically implanted intracortical microelectrodes," *IEEE Trans. Rehabil. Eng.*, vol. 7, no. 3, pp. 315–26, Sep. 1999.

[25] S. Schmidt, K. Horch, and R. Normann, "Biocompatibility of silicon-based electrode arrays implanted in feline cortical tissue," *J Biomed. Mater. Res.*, vol. 27, no. 11, pp. 1393–9, Nov. 1993.

[26] J. C. Williams, R. L. Rennaker, and D. R. Kipke, "Long-term neural recording characteristics of wire microelectrode arrays implanted in cerebral cortex," *Brain Res. Protocols*, vol. 4, pp. 303–313, 1999.

[27] F. Reina-De La Torre, A. Rodriguez-Baeza, and J. Sahuquillo-Barris, "Morphological characteristics and distribution pattern of the arterial vessels in human cerebral cortex: A scanning electron microscope study," *Anat. Rec.*, vol. 251, pp. 87–96, 1998.

[28] D. R. Kipke, R. J. Vetter, J. C. Williams, and J. F. Hetke, "Silicon-substrate intracortical microelectrode arrays for long-term recording of neuronal spike activity in cerebral cortex," *IEEE Trans. Neural Syst. Rehabil. Eng.*, vol. 11, no. 2, pp. 151–155, Jun. 2003.
[29] E. M. Schmidt, M. J. Bak, and J. S. McIntosh, "Long-term chronic recording from cortical neurons," *Exp. Neurol.*, vol. 52, pp. 496–506, 1976.
[30] A. P. Georgopoulos, J. F. Kalaska, R. Kaminiti, and J. T. Massey, "On the relations between the direction of two-dimensional arm movements and cell discharge in primate motor cortex," *J. Neurosci.*, vol. 2, pp. 1527–1537, Nov. 1982.
[31] W. Singer and C. M. Grey, "Visual feature integration and the temporal correlation hypothesis," *Annu. Rev. Neurosci.*, vol. 19, pp. 349–374, 1995.

Selim Suner received the Sc.B. degree with honors in biomedical engineering and artificial organs, the M.S. degree in biomedical engineering, and the M.D. degree, all from Brown University, Providence, RI, in 1986, 1987, and 1992, respectively.

He is an Attending Physician in the Department of Emergency Medicine, Rhode Island Hospital and an Assistant Professor in the Departments of Emergency Medicine and Surgery, Brown Medical School, Providence, RI. He also has expertise in disaster medicine. Since 1998, he has been serving as the Team Leader for the Rhode Island Disaster Medical Assistance Team which is a Department of Homeland Security (DHS) asset under the Federal Emergency Management Agency (FEMA) and the National Disaster Medical System (NDMS). He was awarded the Neuroscience Research Fellowship by the Society for Academic Emergency Medicine in 2003. He is currently editing a textbook, *Disaster Medicine* (St. Louis, MO: Mosby, 2005). His recent research interests include neuromotor prosthesis, local mechanisms of stroke, and management strategies for large disasters involving weapons of mass destruction.

Dr. Suner is a Member of the Society for Neuroscience, Society for Academic Emergency Medicine and has been a Fellow of the American College of Emergency Physicians since 1999.

Matthew R. Fellows received the B.A. degree in microbiology from the University of California, Santa Barbara, in 1994. He is currently working toward the Ph.D. degree in the Neuroscience Department, Brown University, Providence, RI, and is involved in the study of simultaneously recorded neural populations in primate motor cortex.

He was a Research Assistant with the University of California, San Francisco, in a laboratory studying transgenic mouse models of cancer. While there, he developed an interest in systems neuroscience, which led him to the laboratory of John Donoghue at Brown University.

Carlos Vargas-Irwin was born in Cali, Colombia, on September 24, 1979. He received the B.S. degree in neuroscience and the B.A. degree in computer science from Brown University, Providence, RI, in 2002. In 2003, he was granted a Divisional Fellowship and he is currently working toward the Ph.D. degree in the Neuroscience Department, Brown University, conducting research on the representation of movement in the brain since.

.

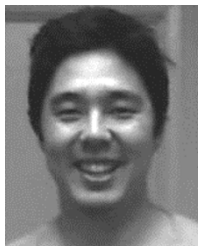

Gordon Kenji Nakata received the B.A. degree in biochemistry from the University of California, Berkeley, in 1992 and the M.D. degree from the State University of New York Health Science Center, Brooklyn, in 1996. He completed the residency in neurological surgery at Brown University, Providence, RI, in 2003.

He is currently an Attending Neurosurgeon in private practice in Eureka, CA.

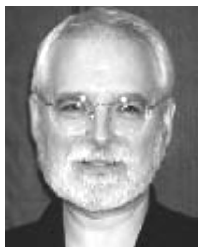

John P. Donoghue (M'03) was born in Cambridge, MA, on March 22, 1949. He received the Ph.D. degree from Brown University, Providence, RI, in 1979.

He is Professor and Chair of the Department of Neuroscience, Brown University, Providence, RI. He has helped develop Brown University's undergraduate neuroscience concentration and the Brain Science Program, which brings together ten departments and more than 100 faculty into a unique interdisciplinary research and education program at Brown University. His personal research program is aimed at understanding how the brain turns thought into movement and the development of neuromotor prosthetic devices. In addition, he is a co-founder of Cyberkinetics, Inc., Foxborough, MA, a biotech startup that is developing brain implants to restore movements to paralyzed individuals.